THE JOURNAL OF PHYSICAL CHEMISTRY A

Article

pubs.acs.org/JPCA

Ab Initio Chemical Kinetics for the Hydrolysis of N_2O_4 Isomers in the Gas Phase

R. S. Zhu,[†] Ke-Yu Lai,[‡] and M. C. Lin*[,†,‡]

[†]Department of Chemistry, Emory University, Atlanta, Georgia 30322, United States

[‡]Center for Interdisciplinary Molecular Science, National Chiao Tung University, Hsinchu 300, Taiwan

Supporting Information

ABSTRACT: The mechanism and kinetics for the gas-phase hydrolysis of N_2O_4 isomers have been investigated at the CCSD(T)/6-311++G(3df,2p)//B3LYP/6-311++G(3df,2p) level of theory in conjunction with statistical rate constant calculations. Calculated results show that the contribution from the commonly assumed redox reaction of *sym*-N_2O_4 to the homogeneous gas-phase hydrolysis of NO_2 can be unequivocally ruled out due to the high barrier (37.6 kcal/mol) involved; instead, *t*-$ONONO_2$ directly formed by the association of $2NO_2$, was found to play the key role in the hydrolysis process.

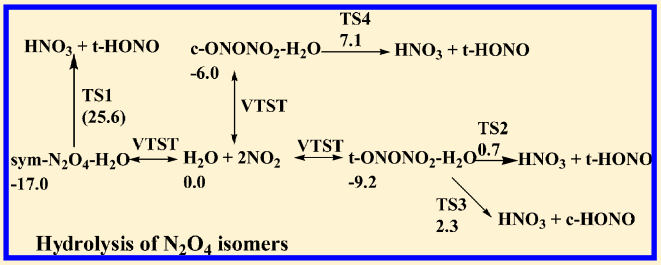

The kinetics for the hydrolysis reaction, $2NO_2 + H_2O \leftrightarrow HONO + HNO_3$ (A) can be quatitatively interpreted by the two step mechanism: $2NO_2 \rightarrow$ *t*-$ONONO_2$, *t*-$ONONO_2 + H_2O \rightarrow HONO + HNO_3$. The predicted total forward and reverse rate constants for reaction (A), $k_{tf} = 5.36 \times 10^{-50} T^{3.95} \exp(1825/T)$ cm^6 molecule^{-2} s^{-1} and $k_{tr} = 3.31 \times 10^{-19} T^{2.478} \exp(-3199/T)$ cm^3 molecule^{-1} s^{-1}, respectively, in the temperature range 200−2500 K, are in good agreement with the available experimental data.

I. INTRODUCTION

Nitrogen oxides play important roles in a wide variety of upper and lower atmospheric systems.[1] Hydrolysis of NO_2 is of particular interest in atmospheric chemistry because it can generate nitrous acid (HONO), a major source of OH in polluted urban atmospheres; the reaction can be represented by reaction A

$$2NO_2 + H_2O \rightarrow HONO + HNO_3 \quad (A)$$

Reaction A, expressed in terms of the two-step mechanism:

$$2NO_2 = N_2O_4 \quad (B)$$

$$N_2O_4 + H_2O = HNO_2 + HNO_3 \quad (C)$$

has been commonly proposed to describe the conversion of nitrogen dioxide to nitric acid in aqueous solution. Experimentally, the heterogeneous formation of HONO in the hydrolysis of NO_2 in water has been extensively studied.[2−11] Most studies show that the rate of absorption of nitrogen dioxide is proportional to the concentration of the dimer of nitrogen dioxide, N_2O_4. Finlayson-Pitts and co-workers proposed a mechanism[7] in which the symmetric N_2O_4 (*sym*-N_2O_4) is formed first, followed by isomerization to $ONONO_2$; the latter reacts with H_2O to form HONO and HNO_3. The kinetics for the homogeneous gas-phase reaction A has been studied by England and Corcoran[12] in the temperature range 298−323 K in N_2 (760 Torr) under highly diluted conditions. The forward and reverse rate constants for reaction A have been measured and reported. Theoretically, several authors[13−16] have investigated N_2O_4 isomeration and its interaction with H_2O from various aspects using density functional theory (DFT) and "on the fly" molecular dynamics calculations at the MP2 level. Chou et al.[13] studied the reaction of symmetric N_2O_4 with water vapor using the DFT method, their results show that the direct production of HONO and HNO_3 needs to overcome more than 30 kcal/mol barrier and the energy barrier is unafected by the presence of multiple water molecules. Pimentel et al.[14] studied the isomerization of *sym*-N_2O_4 to $ONONO_2$ with the combined DFT/B3LYP/13s8p-(2d,1f) level of theory, the isomerization barrier was found to be 31 kcal/mol at 298 K. Miller et al.[15] investigated the ionization of N_2O_4 in contact with water using the on-the-fly molecular dynamics simulation method at the MP2 level; they concluded that ionization of N_2O_4 in and on thin water film surface is a key step in the hydrolysis of NO_2 to form HONO. In the most recent paper of Medeiros and Pimentel,[16] their studies show that NO_2 dimerization and N_2O_4 isomerization in the water-film surface are believed to be the key steps in the hydrolysis of NO_2. However, the initiation mechanism occurring in the atmosphere involving N_2O_4 and H_2O is still poorly understood; no theoretical kinetics calculations have been performed and reported in the literature.

The major objective of this work is to elucidate the gas-phase mechanism for the redox reaction of NO_2 in the presence of H_2O; the roles of the symmetric and asymmetric isomers of N_2O_4 have been studied by careful mapping of the potential energy surface of the system and the rate constants for the

Received: March 7, 2012
Revised: April 16, 2012
Published: April 16, 2012

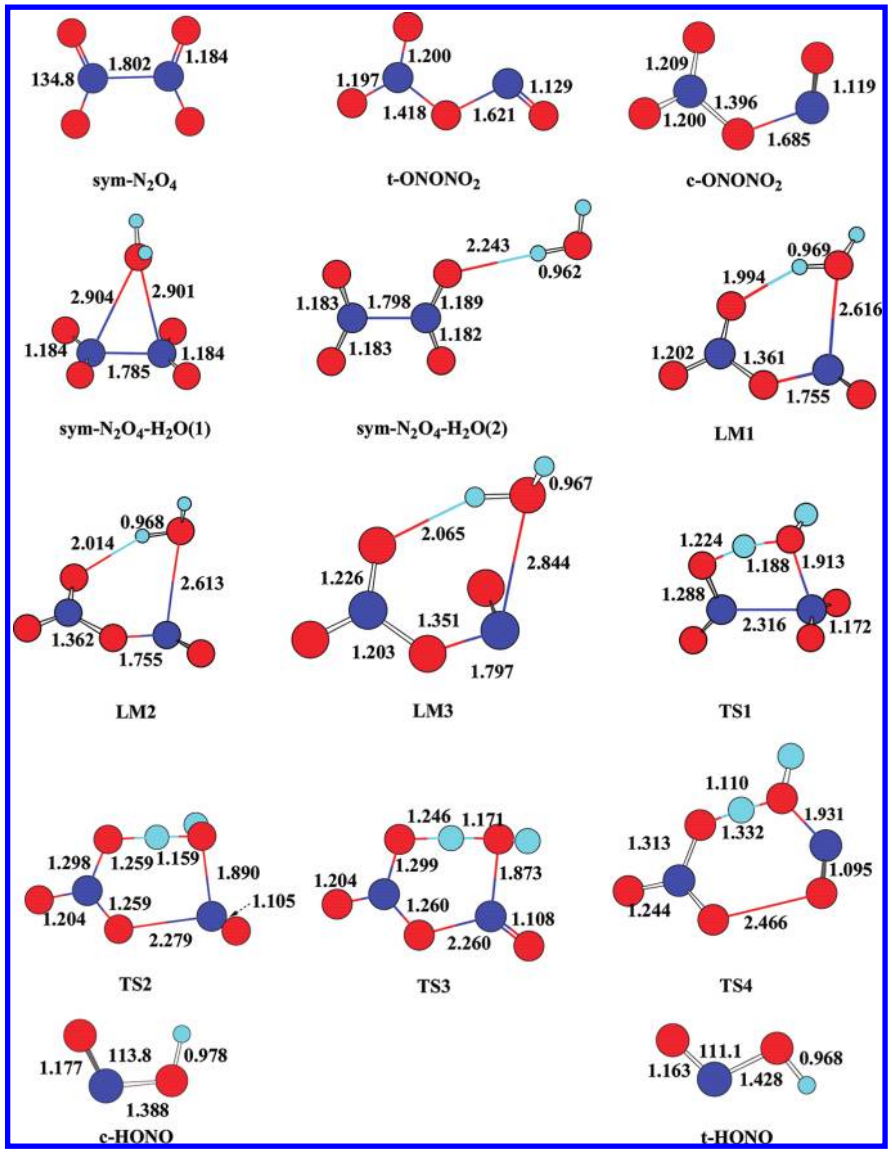

Figure 1. Optimized structures of the reactants, intermediates, and transition states for the reactions of H_2O + *sym*-N_2O_4 and *t*-$ONONO_2$ at the B3LYP/6-311++G(3df,2p) level. The bond lengths are given in angstroms; angles, in degrees.

low-lying energy channels are predicted and compared with the available experimental data. Our result can unequivocally rule out the contribution from the redox reaction of *sym*-N_2O_4 to the homogeneous gas-phase hydrolysis of NO_2.

II. COMPUTATIONAL METHODS

The structures and frequencies of the species involved in the reaction have been fully optimized by using the hybrid density functional (B3LYP) method (i.e., Becke's three-parameter nonlocal exchange functional[17−19] with the correlation functional of Lee, Yang, and Parr[20]) using the standard 6-311++G(3df,2p) basis set. Intrinsic reaction coordinate (IRC) calculations[21] have been performed to confirm the connection of each transition state with designated intermediates and the single point energies were refined at the CCSD(T)/6-311++G(3df,2p) level of theory. All calculations have been carried out using the Gaussian 03 program package.[22]

The third-order rate constant for the hydrolysis reaction, $2NO_2 + H_2O \leftrightarrow HONO + HNO_3$ is interpreted by the two-step mechanism:

$$2NO_2 = ONONO_2 \text{ isomers} \quad (K_{eq})$$

$$ONONO_2 \text{ isomers} + H_2O \leftrightarrow HONO + HNO_3 \quad (k_f)$$

The second-order rate constant k_f has been predicted by the transition state theory (TST)[24] implemented in the Variflex code.[23] Microcanonical Rice−Ramsperger−Kassel−Marcus (RRKM) theory,[24,25] has been used to test the deactivation effect of the complexes. In the RRKM calculations, the L-J parameters, σ = 3.74 Å, ε/κ = 82 K for N_2 are taken from the ref 26; the L-J values for H_2O−$ONONO_2$ complexes, σ = 3.67 and ε/κ = 419 K are derived from those of H_2O (σ = 2.71 Å, ε/κ = 506 K)[26] and N_2O_4 (σ = 4.621 Å, ε/κ = 347 K)[27] using approximation equations of $\sigma(H_2O{-}N_2O_4) = [\sigma(H_2O) + \sigma(N_2O_4)]/2$ and, ε $(H_2O{-}N_2O_4) = [\varepsilon(H_2O)\varepsilon(N_2O_4)]^{1/2}$.

The minimum energy path (MEP) representing the barrierless association processes of H_2O + *t*-$ONONO_2$ is obtained by calculating the potential energy curve along the reaction coordinate O−N bond in the complex LM1 (Figure 1) where the O−N bond length is stretched from the equilibrium value 2.616 to 5.016 Å with an interval step size of 0.2 Å and

dx.doi.org/10.1021/jp302247k | J. Phys. Chem. A 2012, 116, 4466−4472

other geometric parameters are fully optimized. The dissociation curve (see Supporting Information SI-1) can be fitted to the Morse potential function, $E(R) = D_e[1 - \exp(-\beta(R - R_e))]^2$, which is employed to approximate the MEP path for the variational transition state in the rate calculation. In the above equation, R is the reaction coordinate (i.e., the distance between the two bonding atoms; the O−N in this work), D_e is the bond energy excluding zero-point energy, and R_e is the equilibrium value of R (2.616 Å). The computed potential energies can be fitted reasonably to the Morse potential function with the parameter β = 1.763 Å^{-1}. The numbers of states for the tight transition states are evaluated according to the rigid-rotor harmonic-oscillator approximation. The lower vibrational modes in the transition states are treated as classical one-dimensional free rotors in our rate constant calculations. For those paths involving hydrogen atom transfer, Eckart tunneling effects[28,29] were taken into account in the rate constant calculations.

Equilibrium constants were calculated on the basis of $K_p = \exp(-\Delta G/RT)$, where R is the ideal gas law constant with 0.0821 dm^3 atm mol^{-1} K^{-1}; ΔG is the standard Gibbs free energy change, determined by $\Delta H - T\Delta S$, $\Delta H = \sum H_{f,products} - \sum H_{f,reactants}$, which is calculated at the CCSD(T)/6-311++G(3df,2p) level of theory. $\Delta S = \sum S_{products} - \sum S_{reactants}$, which is calculated on the basis of the structural parameters calculated at the B3LYP/6-311++G(3df,2p) level. ΔG values at different temperatures are calculated using the ChemRate program.[30]

III. RESULTS AND DISCUSSION

Several experimental studies[31−34] revealed the existence of asymmetric N_2O_4 isomers besides *sym*-N_2O_4 (D_{2h}). Previous ab initio calculations[35−39] predicted the possible geometries of N_2O_4 isomers. The most stable isomers are *sym*-N_2O_4 and *trans*-ONONO$_2$.[36,39] In this work, the reactions of H_2O with *sym*-N_2O_4, *trans*-ONONO$_2$, and *cis*-ONONO$_2$ have been considered. The structures of the key stationary points and the PES diagram are displayed in Figures 1 and 2, respectively.

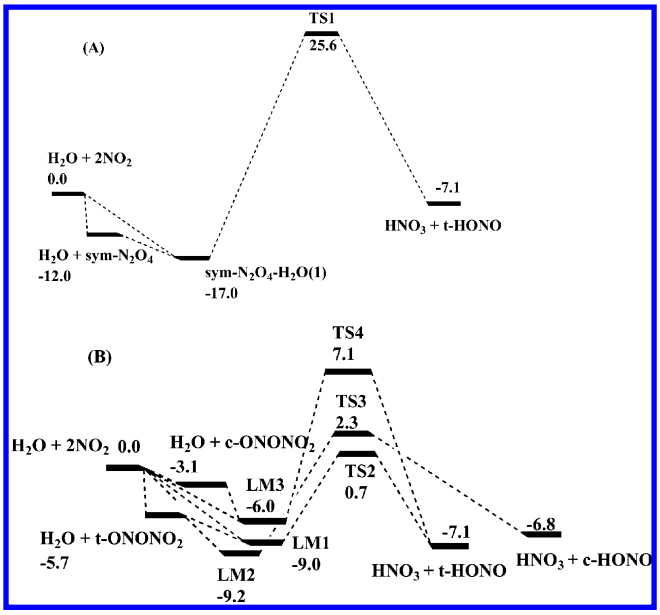

Figure 2. Schematic energy diagrams (in kcal/mol) of H_2O + *sym*-N_2O_4 (A) and *t*-ONONO$_2$ (B), computed at the CCSD(T)/6-311++G(3df,2p)//B3LYP/6- 311++G(3df,2p) level.

The vibrational frequencies and rotational constants are summarized in the Supporting Information (SI-2). To judge the reliability of the coupled clusters approach for this system, the T_1 diagnostics values for the reactants, intermediates, transition states, and products in CCSD(T) were calculated using the 6-311++G(3df,2p) basis set. The data are summarized in Supporting Information SI-3. It can be seen from Supporting Information SI-3 that besides H_2O (T_1 = 0.009), the T_1 values for all other species lie in 0.02 ± 0.004, which are close to the proposed maximum value of 0.02.[40]

For determination of the rate constants from the different mechanisms involving *sym*-N_2O_4 and *t*-ONONO$_2$ given in Figure 2A,B, respectively, we have attempted to scan the MEPs from their intermediates, *sym*-N_2O_4−H_2O (1) and *t*-ONONO$_2$−H_2O (LM1 and LM2), back to their reactants, 2NO_2 + H_2O. The most favorable paths led to *sym*-N_2O_4 + H_2O and *t*-ONONO$_2$ + H_2O because of the much stronger binding between the 2 NO_2 molecules; accordingly, we interpret the termolcular rate constants for 2NO_2 + H_2O on the basis of the two-step mechanism as described by reactions B and C given above for the three isomers as discussed below.

Heats of Reaction and Dissociation Energy. To confirm the reliability of the methods employed, we compared the heats of reaction for this reaction and the dissociation energy for *sym*-N_2O_4 with available experimental values in Table 1. Our

Table 1. Comparison of Calculated Heats of Reaction (kcal/mol) for 2NO_2 + H_2O and D_0 of *sym*-N_2O_4 with the Available Experimental Data

CCSD(T)/6-311++G(3df,2p)[a]	calc (0 K)	expt (0 K)[b]
2NO_2 + H_2O	0.0	
t-HONO + HNO_3	−7.1	−7.2 ± 0.6
c-HONO + HNO_3	−6.8	−6.7 ± 0.6
NO_2 + NO_2	0.0	
sym-N_2O_4	−12.1	−12.7 ± 0.8
t-ONONO$_2$	−5.7	

[a]Based on the optimized structures at the B3LYP/6-311++G(3df,2p) level. [b]Based on the experimental heats of formation (at 0 K) in ref 41.

calculated heats of reaction for the reaction 2NO_2 + H_2O → HNO_3 + *c*-HONO/*t*-HONO, give −6.8 and −7.1 kcal/mol, for the formation of cis- and trans-isomers, respectively; these values are in excellent agreement with the experimental values, −6.7 ± 0.6 and −7.2 ± 0.6 kcal/mol, based on the experimental heats of formation:[41] NO_2 (8.59 ± 0.19 kcal/mo), H_2O (−57.10 ± 0.01 kcal/mol), HNO_3 (−29.75 ± 0.1 kcal/mol), *c*-HONO (−16.85 ± 0.32 kcal/mol), *t*-HONO (−17.36 ± 0.32 kcal/mol). The calculated dissociation energies (D_0) for *sym*-N_2O_4 and *t*-ONONO$_2$ to 2NO_2 are 12.0 and 5.7 kcal/mol, respectively, which are also consistent with the values, 12.4 and 6.2 kcal/mol calculated at the QCISD/6-31+G(2df)//B3LYP/6-31G(d) level.[36] The former is in good agreement with the experimental value, 12.7 ± 0.8 kcal/mol, based on the heats of formation of NO_2 and *sym*-N_2O_4 .[41]

H_2O + *sym*-N_2O_4. Two NO_2 can barrierlessly form *sym*-N_2O_4; then the interaction of H_2O with *sym*-N_2O_4 further forms two complexes, *sym*-N_2O_4−H_2O (1) and *sym*-N_2O_4−H_2O (2), with 5.0 and 1.0 kcal/mol association energies at the CCSD(T)/6-311++G(3df,2p) level, which are consistent with the values, 4.3 and 1.3 kcal/mol, reported by Chou et al.[13] at the B3LYP/6-311+(2d,p) level. Theoretically, the complexes can be formed directly from 2NO_2 + H_2O (Figure 2).

dx.doi.org/10.1021/jp302247k | J. Phys. Chem. A 2012, 116, 4466−4472

sym-N_2O_4–H_2O (1) dissociates to HNO_3 + *trans*-HONO via a five-membered ring transition state TS1 with 37.6 kcal/mol energy above H_2O + *sym*-N_2O_4. At B3LYP/6-311+(2d,p), this barrier was reported to be 32.1 kcal/mol;[13] we believe our value is more reliable because of the larger basis set and the higher level calculation. *sym*-N_2O_4–H_2O (2) has a very shallow well (−1.0 kcal/mol) and the H_2O molecule is just a "spectator" in N_2O_4–H_2O (2), which is not involved in the formation of HONO. The rate constant for the formation of HONO + HNO_3 via *sym*-N_2O_4–H_2O (1) can be represented by

$$k(\text{sym-}N_2O_4 + H_2O) = 7.61 \times 10^{-26} T^{4.53} \exp(-15011/T) \times \text{cm}^3\ \text{molecule}^{-1}\ \text{s}^{-1}$$

in the temperature range 200–2500 K. At 298 K, $k = 5.7 \times 10^{-37}$ cm^3 $molecule^{-1}s^{-1}$. Apparently, the rate is too low for the hydrolysis of N_2O_4 producing HONO + HNO_3 in the gas phase as will be discussed later.

H_2O + *t*-$ONONO_2$. Again, $2NO_2$ can also directly form *t*-$ONONO_2$ with 5.7 kcal/mol association energy (Figure 2B). The interaction of H_2O with *t*-$ONONO_2$ forms two weakly bonded complexes LM1 and LM2 with 3.3 and 3.5 kcal/mol association energies. LM1 and LM2 can dissociate to HNO_3 + *t*-HONO and *c*-HONO products via TS2 and TS3 with 6.4 and 8.0 kcal/mol barriers, respectively, above H_2O + *t*-$ONONO_2$. As one can see, these transition state barriers are about 30.0 kcal/mol lower than that of *sym*-N_2O_4–H_2O system. The fact that *t*-$ONONO_2$ is more reactive than *sym*-N_2O_4 has also been illustrated recently in the hypergolic reaction of N_2H_4 with N_2O_4 isomers.[39]

Rate constants for the following processes are calculated at 760 Torr N_2 pressure in the temperature range 200–2500 K.

$$H_2O + t\text{-}ONONO_2 \rightarrow t\text{-}ONONO_2\text{-}H_2O \quad (k_{as})$$
$$\rightarrow t\text{-HONO} + HNO_3 \quad (k_2)$$
$$\rightarrow c\text{-HONO} + HNO_3 \quad (k_3)$$

The predicted results show that at low temperatures (<280 K), the association process is dominant; with the temperature increasing, the formation of *t*-HONO + HNO_3 becomes competitive and dominant. The calculated individual rate constants are plotted in Figure 3; they can be represented in units of cm^3 $molecule^{-1}$ s^{-1} by the following equations:

$$k_{as.} = 6.49 \times 10^{20} T^{-14.63} \exp(-641/T)$$
$$k_2 = 3.61 \times 10^{-17} T^{1.489} \exp(-2121/T)$$
$$k_3 = 6.96 \times 10^{-18} T^{1.695} \exp(-2775/T)$$
$$k_2 + k_3 = 3.2 \times 10^{-18} T^{1.88} \exp(-2045/T)$$

It should be mentioned that the mechanism involving the isomerization of *sym*-N_2O_4 to $ONONO_2$ is not considered in our calculation due to the high isomeization barrier. For example, at the B3LYP/6-311++G(3df,2p) level, the isomeization barrier is 40.28 kcal/mol; when one H_2O molecule is involved in the isomerization reaction, the barrier is essentially the same, 40.33 kcal/mol, attributable to the factor that the H_2O–N_2O_4 complex and the transition state both are stabilized by the same solvation energy of the added water.

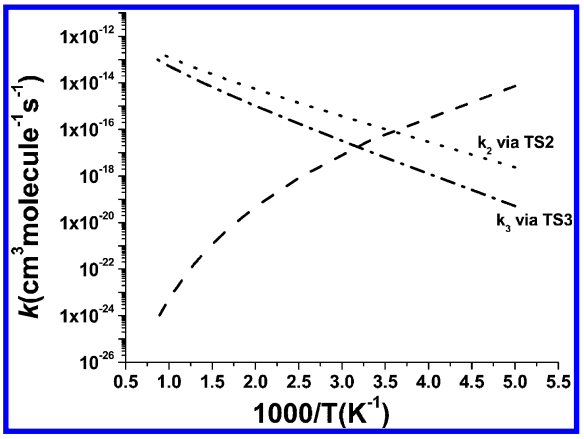

Figure 3. Rate constants for the reaction of H_2O + *t*-$ONONO_2$. The dashed line is the association rate constant for the formation of *t*-$ONONO_2$–H_2O complex; the dash-dotted and dotted lines represent the individual rate constants for the formation of *c*-HONO + HNO_3, *t*-HONO + HNO_3.

H_2O + *c*-$ONONO_2$. Similar calculations have been made for the reaction of *c*-$ONONO_2$ formed by $2NO_2$ with only 3.1 kcal/mol association energy; the reaction with H_2O forms a weak complex (LM3) with a 2.9 kcal/mol binding energy. LM3 can decompose to *t*-HONO + HNO_3 via TS4 with a noticeably higher barrier of 10.2 kcal/mol. The third-order rate constant for the *c*-$ONONO_2$ reaction is shown as a dash-dot-dotted line 4 in Figure 6. As one can see, the lower stability of *c*-$ONONO_2$ and the higher exit barrier of TS4 result in a significantly less contribution to the third-order redox reaction of NO_2 with H_2O, <1% at 298–800 K, comparing with that from the *t*-$ONONO_2$ reaction presented above.

Equilibrium Constant K_A. The predicted K_A is plotted as a solid line in Figure 4, which is in good agreement with the

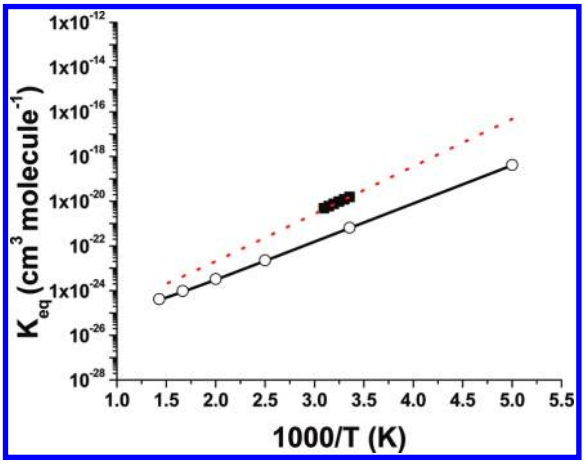

Figure 4. Equilibrium constant for the reaction of $2NO_2$ + H_2O = HONO + HNO_3. Solid and dotted lines are calculated on the basis of the heat of reaction ΔH_r = −7.1 and −9.0 kcal/mol, respectively. ○, calculated on the basis of the ΔG values taken from ref 41; ■, taken from ref 12.

results (given by circles) based on the ΔG values reported in NIST-JANAF Thermochemical Tables.[41] However, our calculated values are lower than those given by England and Corcoran;[12] in their work, the $K_A = k_f/k_r$ where k_f is the experimental third-order rate constant for $2NO_2$ + H_2O and the k_r is the second-order rate constant for the reverse HONO + HNO_3

dx.doi.org/10.1021/jp302247k | J. Phys. Chem. A 2012, 116, 4466–4472

reaction. Based on their K_A, the heat of reaction at 298 K is 1.9 kcal/mol lower than ours; using their heat of reaction and our predicted geometric parameters, the calculated values (given by dotted line in Figure 4) can reproduce their reported data.

Rate Constant for HONO + HNO_3. On the ground that the bimolecular reaction HONO + HNO_3 via TS1 producing *sym*-N_2O_4 has a significantly higher barrier, only the rate constants for the low-energy channels via TS2, TS3, and TS4 have been calculated. In these reverse reactions, the deactivation rates for the excited intermediates LM1−LM3 can be reasonably ignored as they can readily dissociate to H_2O + *t*-$ONONO_2$ (or H_2O + $2NO_2$) and H_2O + *c*-$ONONO_2$ (or H_2O + $2NO_2$). Accordingly, the conventional TST[24] was used to calculate the rate constants for these reverse reaction channels with Eckart tunneling corrections.[28,29] k_{tr} is the sum of the individual rates via TS2, TS3, and TS4. The negligible deactivation effects have been confirmed by our RRKM calculation. At 760 Torr N_2, 100% of activated complexes barrierlessly dissociate to H_2O + *t*-$ONONO_2$ in the range of 200−2500 K, followed by the rapid fragmentation of *t*-$ONONO_2$ to $2NO_2$ with only 5.7 kcal/mol dissociation energy.

The predicted result is plotted and compared with available experimental values in Figure 5. Our calculated individual and total rate constants can be represented in units of cm^3 $molecule^{-1}$ s^{-1} by

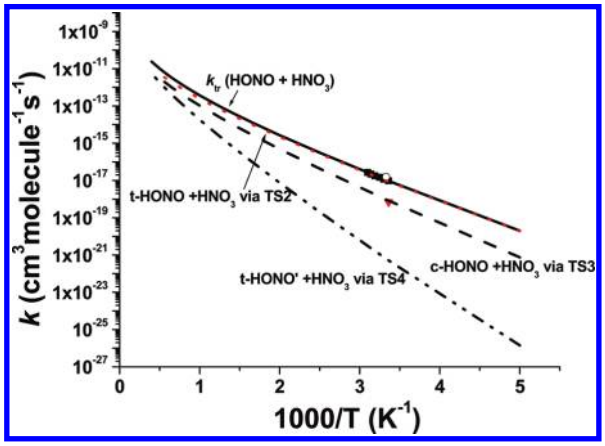

Figure 5. Rate constants for the reaction of HONO + HNO_3. Dashed, dotted, and dash-dot-dotted lines represent the calculated values of k(*c*-HONO + HNO_3) via TS3, k(*t*-HONO + HNO_3) via TS2, and k(*t*-HONO′ + HNO_3) via TS4; the solid line is the total rate, k_{tr}(HONO + HNO_3); symbols are the experimental values: ■, ref 12; ○, ref 42; ▼, ref 43.

$$k(c\text{-HONO} + HNO_3) = 1.28 \times 10^{-18} T^{2.186} \exp(-3816/T) \text{ via TS3}$$

$$k(t\text{-HONO} + HNO_3) = 3.32 \times 10^{-18} T^{2.092} \exp(-3253/T) \text{ via TS2}$$

$$k(t\text{-HONO}' + HNO_3) = 2.78 \times 10^{-19} T^{2.465} \exp(-5987/T) \text{ via TS4}$$

$$k_{tr}(\text{HONO} + HNO_3) = 3.31 \times 10^{-19} T^{2.478} \exp(-3199/T)$$

Figure 5 shows that in the whole temperature range, the reaction of *t*-HONO + HNO_3 via TS2 is dominant. At 298 K, k_{tr}(HONO + HNO_3) = 1.04×10^{-17} cm^3 $molecule^{-1}$ s^{-1}, which is in good agreement with the experimental values, 1.18×10^{-17} (ref 12) and 1.55×10^{-17} cm^3 $molecule^{-1}s^{-1}$ (ref 42). However, the value measured by Wallington and Japar,[43] 7.01×10^{-19} cm^3 $molecule^{-1}$ s^{-1}, although in agreement with our predicted result for the *c*-HONO + HNO_3 reaction, 9.34×10^{-19} cm^3 $molecule^{-1}s^{-1}$, is lower than the predicted total rate.

Third-Order Rate Constant for $2NO_2$ + H_2O. In the work of England and Corcoran,[12] the experimentally measured third-order rate constant for the homogeneous gas-phase hydrolysis reaction, $2NO_2$ + H_2O → HONO + HNO_3 (A), was interpreted according to the two-step mechanism: $2NO_2$ → *sym*-N_2O_4 (B) and *sym*-N_2O_4 + H_2O→ HONO + HNO_3 (C) as alluded to above. On the basis of this mechanism, we can theoretically calculate the equilibrium constant and the second-order rate constant for the above reactions, denoted as K_{eq}(*sym*-N_2O_4) and k(*sym*-N_2O_4 + H_2O), employing our quantum chemically predicted energetics and molecular parameters. The third-order rate constant can be given by $k_f = K_{eq}$(*sym*-N_2O_4) × k(H_2O + *sym*-N_2O_4); the computed result is presented by the dotted line in Figure 6. From the figure, one can see that in the experimental temperature range, the calculated k_f is more than 10 orders of magnitude lower than the experimental data reported by England and Corcoran,[12] attributable to the high barrier at TS1 (37.6 kcal/mol) for the formation of HONO + HNO_3 from the *sym*-N_2O_4 + H_2O reaction. Therefore, the role of *sym*-N_2O_4 in the formation of HONO + HNO_3 can be ignored.

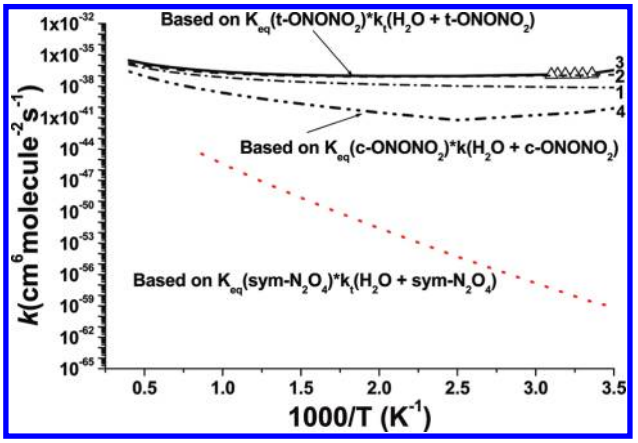

Figure 6. Third-order rate constants for the reaction of $2NO_2$ + H_2O → HONO + HNO_3, calculated on the basis of the mechanism of $2NO_2$ = *t*-$ONONO_2$; H_2O + *t*- $ONONO_2$ = HONO + HNO_3. Dash-dotted line 1, dashed line 2, and solid line 3 represent the individual rate constants for the formation of *c*-HONO + HNO_3, *t*- HONO + HNO_3, and the total rate k_{tf}. Dash-dot-dotted line 4 is calculated on the basis of the mechanism of $2NO_2$ = *c*-$ONONO_2$; H_2O + *c*-$ONONO_2$ = *t*-HONO + HNO_3. The dotted line is calculated on the basis of the mechanism of $2NO_2$ = *sym*-N_2O_4; H_2O + *sym*-N_2O_4 = HONO + HNO_3. Δ, experimental values taken from ref 12.

On the other hand, if we assume that the third-order redox reaction of NO_2 with H_2O involves primarily the reaction of *t*-$ONONO_2$ with H_2O, we can use the following reaction mechanism as depicted by the PES in Figure 2B to interpret England and Corcoran's experimental data:

$$2NO_2 \leftrightarrow t\text{-}ONONO_2$$

$$t\text{-}ONONO_2 + H_2O \rightarrow HONO + HNO_3$$

dx.doi.org/10.1021/jp302247k | J. Phys. Chem. A 2012, 116, 4466−4472

Table 2. Summary of Calculated and Experimental Forward and Reverse Rate Constants for the Reaction of $2NO_2 + H_2O \leftrightarrow HNO_2 + HNO_3$ (A)

T (K)	calc, k_{tf}[a]	calc, k_{tr}[b]	T (K)	expt,[c] k_{tf}	expt,[c] k_{tr}
300	1.49×10^{-37}	1.04×10^{-17}	298	1.52×10^{-37}	9.71×10^{-18} (7.01×10^{-19})[d]
400	9.63×10^{-38}	3.09×10^{-16}	303	1.44×10^{-37}	1.18×10^{-17} [1.55×10^{-17}][e]
500	9.62×10^{-38}	2.68×10^{-15}	308	1.41×10^{-37}	1.47×10^{-17}
600	1.08×10^{-37}	1.23×10^{-14}	313	1.36×10^{-37}	1.79×10^{-17}
700	1.28×10^{-37}	3.85×10^{-14}	318	1.33×10^{-37}	2.21×10^{-17}
800	1.57×10^{-37}	9.51×10^{-14}	323	1.30×10^{-37}	2.69×10^{-17}
1000	2.41×10^{-37}	3.69×10^{-13}			
1200	3.68×10^{-37}	9.90×10^{-13}			
1500	6.60×10^{-37}	2.94×10^{-12}			
1800	1.10×10^{-36}	6.58×10^{-12}			
2000	1.50×10^{-36}	1.02×10^{-12}			
2500	2.94×10^{-36}	2.38×10^{-11}			

[a]In unit of cm^6 $molecule^{-2}$ s^{-1}. [b]in unit of cm^3 $molecule^{-1}$ s^{-1}. [c]Reference 12. [d]Reference 43. [e]Reference 42.

Similar to the above calculation, the forward third-order rate constant k_f for $2NO_2 + H_2O$ can be computed by $K_{eq}(t\text{-}ONONO_2) \times k(H_2O + t\text{-}ONONO_2)$, where $K_{eq}(t\text{-}ONONO_2)$ is the equilibrium constant for $2NO_2 \leftrightarrow t\text{-}ONONO_2$; the values for $k(H_2O + t\text{-}ONONO_2)$ have been calculated and presented in Figure 3 as k_2 and k_3. The individual forward rate constants [$k(t\text{-}HONO)$ and $k(c\text{-}HONO)$] for $2NO_2 + H_2O$ producing $t\text{-}HONO + HNO_3$ and $c\text{-}HONO + HNO_3$ are calculated by $k(t\text{-}HONO) = K_{eq}(t\text{-}ONONO_2) \times k_2$ and $k(c\text{-}HONO) = K_{eq}(t\text{-}ONONO_2) \times k_3$, respectively, and $k_{tf} = k(t\text{-}HONO) + k(c\text{-}HONO)$.

The calculated total k_{tf} is summarized in Table 2 to compare with available experimental data. The individual and total rate constants given in units of cm^6 $molecule^{-2}$ s^{-1} are also shown in Figure 6; they can be represented by

$$k(c\text{-}HONO) = 2.72 \times 10^{-49} T^{3.670} \exp(951/T)$$

$$k(t\text{-}HONO) = 6.80 \times 10^{-47} T^{3.565} \exp(1654/T)$$

$$k_{tf} = 5.36 \times 10^{-50} T^{3.95} \exp(1825/T)$$

in the temperature range 300−2500 K. Calculated results in Figure 6 show that the formation of $t\text{-}HONO + HNO_3$ is dominant in the whole temperature range computed; the predicted total k_{tf} values are in good agreement with the experimental data of England and Corcoran.[12] In the temperature of range 300−500 K, k_{tf} exhibits a small negative T-dependent because the decrease in the value of $K_{eq}(t\text{-}ONONO_2)$ with temperature is larger than the increase rate of $k(H_2O + t\text{-}ONONO_2)$, fully consistent with the experimental observation.

IV. CONCLUSIONS

The gas-phase mechanism and kinetics for the reaction of $2NO_2 + H_2O$ have been elucidated at the CCSD(T)/6-311++G(3df,2p)//B3LYP/6-311++GH(3df,2p) level aided by statistical theory calculations. Our predicted results show that the termolecular reaction of $2NO_2$ with H_2O can directly form *sym*-N_2O_4−H_2O, $t\text{-}ONONO_2$−H_2O, and $c\text{-}ONONO_2$−H_2O complexes with 17.0, 9.0/9.2, and 6.0 kcal/mol association energies, respectively. Further transformation of these complexes by undergoing intramolecular redox reactions giving rise to $HONO + HNO_3$ requires 42.6 kcal/mol activation energy at TS1 for the *sym*-N_2O_4−H_2O complex and only 9.7, 11.5, and 13.1 kcal/mol at TS2, TS3, and TS4 for LM1, LM2 ($t\text{-}ONONO_2$−H_2O complexes), and LM3 ($c\text{-}ONONO_2$−H_2O complex). The existing experimental results for the hydrolysis reaction, $2NO_2 + H_2O \rightarrow HONO + HNO_3$, can be quantitatively accounted for primarily by the two-step mechanism: $2NO_2 \rightarrow t\text{-}ONONO_2$, $t\text{-}ONONO_2 + H_2O \rightarrow HONO + HNO_3$. Our finding may help understand the mechanism for the absorption of nitrogen dioxide into aqueous solution. A comparison of the gas phase with the aqueous solution kinetics for this important system will be investigated in the near future.

■ ASSOCIATED CONTENT

Supporting Information

SI-1, the dissociation curve of $t\text{-}ONONO_2$−H_2O complex; SI-2, the vibrational frequencies and rotational constants for the intermediates, transition states, and products in the reactions of $2NO_2 + H_2O$, computed at the B3LYP/6-311+G(3df,2p) level of theory; SI-3, the T1 diagnostics for the reactants, intermediates, transition states, and products in the reactions of $2NO_2 + H_2O$, computed at the CCSD(T)/6-311++G(3df,2p) level of theory. Complete citation for ref 22. This material is available free of charge via the Internet at http://pubs.acs.org

■ AUTHOR INFORMATION

Corresponding Author

*E-mail: chemmcl@emory.edu.

Notes

The authors declare no competing financial interest.

■ ACKNOWLEDGMENTS

We are grateful to Taiwan's National Center for High-performance Computing for the CPU and to Taiwan's National Science Council for a research stipend to K.Y.L. and to M.C.L. for a Distinguished Visiting Professorship at the National Chiao Tung University in Hsinchu, Taiwan. R.S.Z. thanks ONR (N00014-08-1-0106) for the support of this work at Emory University.

■ REFERENCES

(1) Finlayson-Pitts, B. J.; Pitts, J. N., Jr. *Chemistry of upper and Lower Atmosphere: Theory, Experiments and Application*; Academic Press: New York, 2000.

(2) Platt, U; Perner, D.; Harris, G. W.; Winer, A. M.; Pitts, J. N., Jr. *Nature* **1980**, *285*, 312.
(3) Calvert, J. G.; Yarwood, G.; Dunker, A. M. *Res. Chem. Intermed.* **1994**, *20*, 463.
(4) Kotamarthi, V. R.; Gaffney, J. S.; Marley, N. B.; Doskey, P. V. *Atmos. Environ.* **2001**, *35*, 4489.
(5) Stutz, J.; Alicke, B.; Neftel, A. *J. Geophys. Res. Atmos.* **2002**, *107*, 8192.
(6) Perner, D.; Platt, U. *Geophys. Res. Lett.* **1979**, *6*, 917.
(7) Finlayson-Pitts, B. J.; Wingen, L. M.; Sumner, A. L.; Syomin, D.; Ramazan, K. A. *Phys. Chem. Chem. Phys.* **2003**, *5*, 223.
(8) Barney, W. S.; Finlayson-Pitts, B. J. *J. Phys. Chem. A* **2000**, *104*, 171.
(9) Carter, W. P. L; Atkinson, R.; Winer, A. M.; Pitts, J. N. *Int. J. Chem. Kinet.* **1981**, *13*, 735.
(10) Lammel, G.; Cape, J. N. *Chem. Soc. Rev.* **1996**, *25*, 361.
(11) Ramazan, K. A.; Wingen, L. M.; Miller, Y.; Chaban, G. M.; Gerber, R. B.; Xantheas, S. S.; Finlayson-Pitts, B. J. *J. Phys. Chem. A.* **2006**, *110*, 6886.
(12) England, C.; Corcoran, W. H. *Ind. Eng. Chem. Fundam.* **1974**, *13*, 373.
(13) Chou, A.; Li, Z. R.; Tao, F. M. *J.Phys. Chem. A* **1999**, *10*, 7848.
(14) Pimentel, A. S.; Lima, F. C. A.; da Silva, A. B. F. *J. Phys. Chem. A* **2007**, *111*, 2913.
(15) Miller, Y.; Finlayson-Pitts, B. J.; Gerber, R. B. *J. Am. Chem. Soc.* **2009**, *131*, 12180.
(16) MedeirosDiogo de Jesus, Diogo de Jesus; Pimentel, Andre Silva. *J. Phys. Chem.* **2011**, *115*, 6357.
(17) Becke, A. D. J. *Chem. Phys.* **1993**, *98*, 5648.
(18) Becke, A. D. J. *Chem. Phys.* **1992**, *96*, 2155.
(19) Becke, A. D. J. *Chem. Phys.* **1992**, *97*, 9173.
(20) Lee, C.; Yang, W.; Parr, R. G. *Phys. Rev.* **1988**, *B37*, 785.
(21) Gonzalez, C.; Schlegel, H. B. *J. Phys. Chem.* **1989**, *90*, 2154.
(22) Frisch, M. J.; Trucks, G. W.; Head-Gordon, M.; Gill, P. M. W.; Wong, M. W.; Foresman, J. B.; Johnson, B. G.; Schlegel, H. B.; Robb, M. A.; Replogle, E. S. et al. *Gaussian 92/DFT*, Revision B; Gaussian, Inc.: Pittsburgh, PA, 2003.
(23) Klippenstein, S. J.; Wagner, A. F.; Dunbar, R. C.; Wardlaw, D. M. Robertson, S. H. *VARIFLEX*, VERSION 1.00, 1999.
(24) Gilbert, R. G.; Smith, S. C. *Theory of Unimolecular and Recombination Reactions*; Blackwell Scientific: Carlton, Australia, 1990.
(25) Troe, J. *J. Chem. Phys.* **1977**, *66*, 6745.
(26) Hippler, H.; Troe, J.; Wendelken, H. J. *J. Chem. Phys.* **1983**, *76*, 6709.
(27) Cressault, Y.; Connord, V.; Hingana, H.; Teulet, Ph.; Gleizes, A. *J. Phys. D: Appl. Phys.* **2011**, *44*, 495202.
(28) Eckart, C. *Phys. Rev* **1930**, *35*, 1303.
(29) Hase, W. L. Baer *Unimolecular Reaction Dynamics*; International Series of Monographs on Chemistry; Oxford University Press: New York, 1996.
(30) Mokrushin, V.; Bedanov, V.; Tsang, W.; Zachariah, M. R.; Knyazev, V. D. *ChemRate*, Version 1.19; National Institute of Standards and Technology: Gaithersburg, MD, 2002.
(31) Givan, A.; Loewenschuss, A. *J. Chem. Phys.* **1989**, *90*, 6135.
(32) Givan, A.; Loewenschuss, A. *J. Chem. Phys.* **1989**, *91*, 5126.
(33) Givan, A.; Loewenschuss, A. *J. Chem. Phys.* **1991**, *94*, 7562.
(34) Pinnick, D. A.; Agnew, S. F.; Swanson, B. I. *J. Phys. Chem.* **1992**, *96*, 7092.
(35) Stirling, A.; Papai, I.; Mink, J.; Salahub, D. R. *J. Chem. Phys.* **1994**, *100*, 2910.
(36) McKee, M. L. *J. Am. Chem. Soc.* **1995**, *117*, 1629.
(37) Zakharov, I. I.; Kolbasin, A. I.; Zakharova, O. I.; Kravchenko, I. V.; Dyshlovoi, V. I. *Theor. Exp. Chem.* **2008**, *44*, No.1, 26−31.
(38) Wang, X.; Qin, Q.-Z.; Fan, K. *J. Mol. Struct. (THEOCHEM)* **1998**, *432*, 55.
(39) Lai, K-Y; Zhu, R. S.; Lin, M. C. *Chem. Phys. Lett.* **2012**, In press.
(40) Lee, T.J. Lee; Taylor, P. R. *Int. J. Quantum Chem.* **1989**, *S23*, 199.
(41) Chase, Jr. M. W. *NIST-JANAF Thermochemical Tables*, 4th ed.; Woodbury, NY, 1998.
(42) Kaiser, E. W.; Wu, C. H. *J. Phys. Chem.* **1977**, *81*, 187.
(43) Wallington, T. J.; Japar, S. M. *J. Atmos. Chem.* **1989**, *9*, 399.